Effect of anisotropy on the instability of crack propagation

Péter Szelestey,[1,2] Pekka Heino,[2,*] János Kertész,[1,2] and Kimmo Kaski[2]
[1]*Department of Theoretical Physics, Institute of Physics, Technical University of Budapest, 8 Budafoki út, H-1111 Budapest, Hungary*
[2]*Laboratory of Computational Engineering, Helsinki University of Technology, P.O. Box 9400, FIN-02015 HUT, Finland*
(Received 6 July 1999)

Dynamics of fracture is investigated in an anisotropic two-dimensional Born-Maxwell model by numerical simulations. From previous studies it is known that the isotropic model shows crack branching and velocity oscillations of the propagating main crack above a critical velocity, similarly with experimental findings in some brittle materials. Here we present studies in which anisotropy has been introduced to the model system. Anisotropy is found to have significant effects on crack propagation and on the pattern it forms. In the case of symmetric anisotropy (relative to the crack direction) we found changes in velocity oscillation and side branching properties. In the case of asymmetric anisotropy two kinds of periodicities occur and strong anisotropy causes different branch patterns to form at two sides of the main crack. In addition, the role of disorder through distributed spring constants has been studied for both types of anisotropy. Finally a simple exactly solvable model for investigating the initial stages of crack branching has been developed and analyzed.

PACS number(s): 62.20.Mk, 83.50.Tq, 02.70.Ns

I. INTRODUCTION

Fracture behavior of materials has been under active research for a long time. Traditionally it has been treated by the material scienctists and engineers for its obvious technological importance in various applications. In addition, from the physics point of view fracture and more specifically crack dynamics is interesting also because of the rich variety of patterns that form and due to its connection to growth models [1–3].

A long-standing problem, which is still not fully understood, has been how to theoretically explain the experimental observations of crack propagation velocity in some brittle materials [4,5]. Ordinary continuum theory predicts that the crack propagates with the sonic speed of the free surface, which is called Rayleigh wave speed. However, experiments show that the crack tip velocity, at least in amorphous brittle materials, is significantly less than the Rayleigh speed. Since the early 1950s there has been many attempts to explain this contradiction and it was Yoffe [6] who first predicted through the continuum theoretical approach the crack propagation velocity to be 0.6 times the Rayleigh wave speed.

In their experiments on glass and poly(methyl methacrylate) (PMMA) Fineberg *et al.* [7] observed oscillations in the crack tip velocity above a certain limiting speed, which is one-third of the theoretical limit. Later Sharon *et al.* [8] pointed out that the correlation of crack branching with velocity oscillations of the propagating main crack is responsible for the observed low crack velocity. Recent experiments of Boudet *et al.* [9] have shown that it is not necessary that velocity oscillations and branching are directly connected, and that the phenomenon is more complex than previously thought. Beside the experiments and theoretical works [10,11], computer simulations [12–14] play an important role for better understanding of the complexity and instability occuring in brittle fracture.

In this study our main motivation has been to determine how anisotropy and disorder influence the crack branching instability, and to characterize and understand these effects. We are going to do this within the framework of a phenomenological and parametrized dynamical model that includes elastic and plastic or viscous features as well as disorder at the bond level. In spite of these simplifying assumptions we believe that our model—though qualitative—is sufficient in describing some of the salient features real anisotropic systems show.

II. MODEL

In our numerical simulations we have used a classical viscoelastic Born-Maxwell model with the triangular lattice symmetry (Fig. 1). The Born model [15,16] consists of mass points and bonds that connect the nearest neighbor sites. Each bond is described with two spring constants α and β representing the tensile and bending stiffnesses of the bond, respectively. Although the Born model is not rotationally invariant, fracture under mode-I loading can be described quite well, since the rotations of bonds in the system are small. In the model the potential energy of a bond between the sites i and j is defined in the following way:

$$H_{ij}=\frac{\alpha}{2}[(\vec{u}_i-\vec{u}_j)\cdot\vec{d}_{i,j\parallel}]^2+\frac{\beta}{2}[(\vec{u}_i-\vec{u}_j)\cdot\vec{d}_{i,j\perp}]^2, \qquad (1)$$

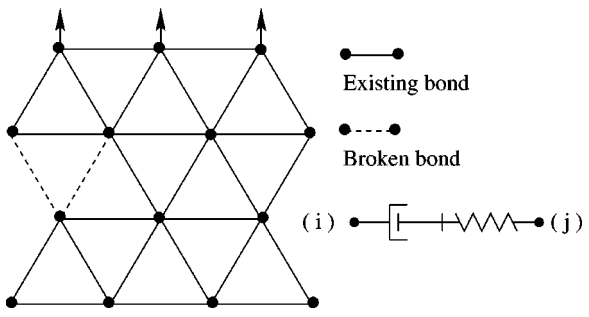

FIG. 1. Born-Maxwell model.

*Present address: Tampere University of Technology, P.O. Box 692, FIN-33101, Tampere, Finland.

where u_i denotes the displacement of mass site i from its initial position, $\vec{d}_{i,j\perp}$ and $\vec{d}_{i,j\parallel}$ are unit vectors connecting sites i and j at $t=0$. Since the constant α is related to the Young modulus, and β to the shear modulus, the ratio α/β is related to the Poisson ratio [13,17]. During the simulation procedure the ratio α/β was kept always the same in the anisotropic as well as in the disordered case. It is noted that the mass sites do not represent individual atoms but pieces of material at a mesoscopic scale, ranging from nanometer up to millimeter scale.

Our model also bears viscoelastic behavior as a simple extension of ideal elasticity. It describes materials in which stress decreases exponentially with time. Thus viscosity has the consequence that there exists dissipation in the bulk, and in addition there appears attenuation of (acoustic or shock) waves. This has the effect of decreasing the role of finite size in our simulation studies. The viscoelastic property is included in the model in a manner introduced by Rautiainen *et al.* [18] and further discussed by Heino and Kaski [13]. It is assumed that relative displacements of mass points can be decomposed into elastic and viscous parts, which means that a bond between two nearest neighbor mass points consists of a simple Born spring and a Newton-type viscous element connected in a series with the spring. Denoting the elastic displacement of mass site j from its initial position by $\vec{u}_{e,j}$ one writes the equation of motion of the mass site in the following form:

$$m_j\ddot{\vec{u}}_j=\sum_{i\in nn_j}\{\alpha[(\vec{u}_{e,i}-\vec{u}_{e,j})\cdot\vec{d}_{i,j\parallel}]\vec{d}_{i,j\parallel} + \beta[(\vec{u}_{e,i}-\vec{u}_{e,j})\cdot\vec{d}_{i,j\perp}]\vec{d}_{i,j\perp}\}, \tag{2}$$

$$\dot{\vec{u}}_{e,j}=\dot{\vec{u}}_j-\frac{1}{\tau}\vec{u}_{e,j}. \tag{3}$$

Here (2) is the equation of motion, where forces are caused by elastic displacements, and (3) describes dissipation, which connects the elastic and total displacement vectors. With appropriate boundary and initial conditions they fully describe the dynamics of the system. The details of the derivations are omitted here and interested readers can find them in Ref. [13]. For computational simplicity the lattice constant and masses of lattice sites were chosen to unity. The spring constants were chosen to be $\alpha=500$ and $\beta=250$ unless otherwise specified. In the simulations the set of equations (2) and (3) have been solved numerically with the fourth order Runge-Kutta method by using sufficiently small integration time ($\Delta t=0.001$), such that decreasing the value of Δt does not affect the results any longer.

Initially we introduce a crack seed by cutting a small number of bonds (before applying loading at $t=0$) in the center of the left side of the sample to control the direction of the crack line. The length of the notch in the horizontal direction was chosen to be 10 lattice constants long. This left side and the parallel right side of the model system were free so that we used free boundary conditions. In the simulations mode-I loading was applied, i.e., the loading is imposed to the system by moving the topmost row of mass sites in the y direction and the bottom-most row of mass sites was kept fixed. The rate of loading was kept constant $v_s=0.01$ during the simulations except an initial period ($0<t<T_i$) in which the topmost row was moved smoothly with the time dependent rate $2T_iv_s/\pi[1-\cos(t/T_i)(\pi/2)]$, to minimize the generation of sound waves. A bond in the system under external loading was ruptured irreversibly and instantly when the relative distance of mass points exceeded the chosen rupture threshold of 1% above the original equilibrium (unit) length of the bond. In our simulations a typical system consisted of 300×100 mass points. The relaxation parameter was chosen $\tau=25$. For the strain rate used here this describes moderate dissipation [18].

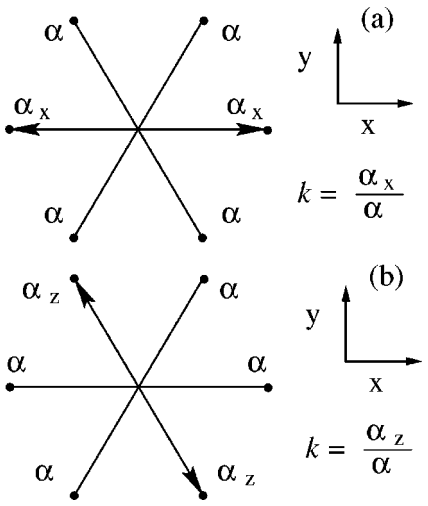

FIG. 2. Special directions in the case of (a) symmetric and (b) asymmetric anisotropy.

III. NUMERICAL SIMULATIONS

Results in an isotropic system [13] show that initially, the crack tip advances straight with increasing velocity. After reaching a critical value, daughter cracks emerge to both sides of the main crack. As a result the mirror-type fracture pattern changes to mist. In connection to branching there are large oscillations in the velocity of the propagating main crack. Both the main and daughter cracks appear straight and the mean velocity of the crack tip has a very slightly increasing trend.

For simplicity the ordered system is treated first. In such a system anisotropy means that the material properties depend on the direction they are measured in the model. In this case anisotropy is introduced by choosing the spring constants α and β different for different orientations. Two cases were studied: symmetric and asymmetric. In the symmetric case horizontal bonds have different elastic constants from the other bonds. In the asymmetric case bonds that form the angle of 60° with the horizontal direction have different elastic constants. The strength of the anisotropy is described by an anisotropy constant k, which is the ratio of the spring constant in the special direction (horizontal in the symmetric and 60° angle in the asymmetric case) with the spring constant in the other direction $k=\alpha_{spec}/\alpha=\beta_{spec}/\beta$.

A. Symmetric anisotropy

In the case of symmetric anisotropy the special direction is parallel to the main crack [Fig. 2(a)]. We have done the

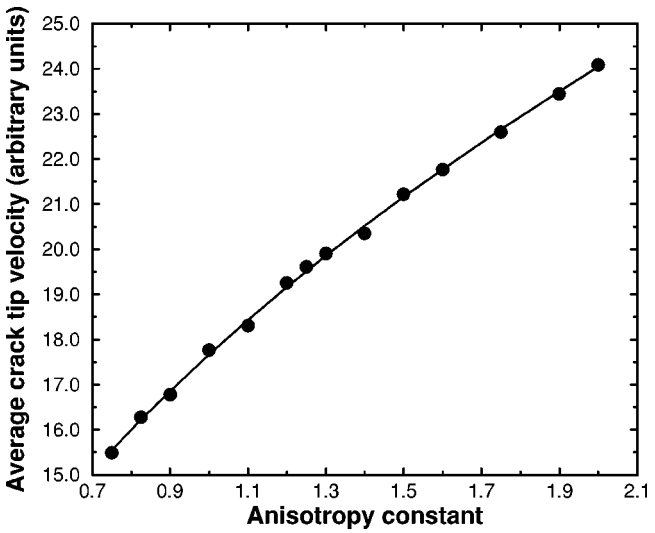

FIG. 3. Dependence of average crack tip velocity on anisotropy constant. The solid line represents the power-law fitted curve.

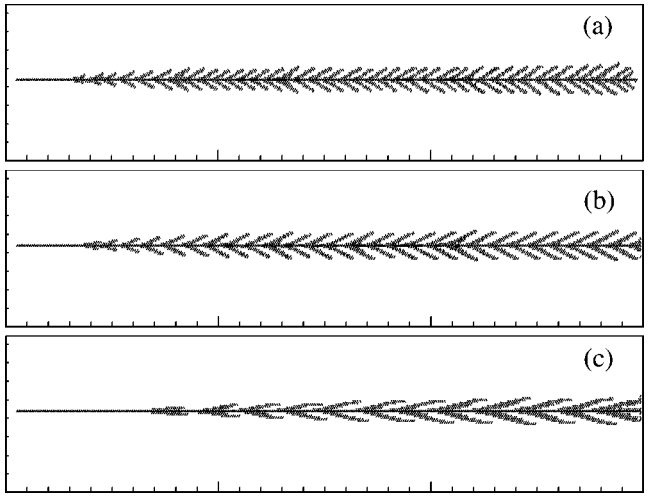

FIG. 4. Fracture pattern in case of symmetric anisotropy. Patterns for system with (a) $k=0.825$, (b) $k=1$, and (c) $k=2.0$, respectively, are shown.

simulations in the interval of the anisotropy constant $0.5<k<2.2$. The average speed of the main crack, the spatial periodicity of daughter cracks, and the frequency of velocity oscillations were closely investigated.

Focusing first on the crack velocity we find that increasing the anisotropy constant means an increase in the critical velocity and also in the average speed level of the periodic part of the velocity vs time plot. Since in this model the speed of sound depends on the spring constants, and in case of the chosen special direction, parallel with the direction of the main crack, it is $v_{\text{sound}}=\sqrt[4]{(\alpha k)^2+(\beta k)^2}$, and the average crack velocity is related to it, one might expect the following square root dependence on the anisotropy, $v_{\text{crack}}\sim\sqrt{k}$. For comparison we have determined the crack velocity from the simulations as a function of k and fitted it to the form $v_{\text{crack}}\sim k^z$. As shown in Fig. 3 we get for the exponent the value $z=0.44$, which is near the expected value of $\frac{1}{2}$, though outside the error bars (about ± 0.005) of the nonlinear regression used in the fitting. This deviation may be due to subtle finite size effects.

In the simulations we have found that the main impact of anisotropy on the fracture pattern is that if we increase the anisotropy constant k, longer daughter cracks will appear while the angle between the main crack and daughter cracks decreases, as can be seen in Fig. 4. This angle changes from 37° for $k=0.825$ to 17° for $k=2.0$. Also in the case of larger anisotropy the period between branchings increases, which is due to the fact that it takes time for the crack tip to accelerate and reach the critical velocity value for crack branching to occur. Our simulations also show that in the model the growth of daughter cracks is stopped if their vertical distance from the main crack reaches a certain value. We have found this value to be independent of the value of anisotropy. On the other hand, it is seen that the apparent width of the fracture pattern, i.e., the extent around the main crack, depends on the strain rate and the strength of viscosity [13]. It has been found that increasing the viscosity (i.e., descreasing τ) decreases the length of daughter cracks, while a faster loading rate increases their lengths. The shape of the daughter cracks are straight and no evidence of bending, i.e., curving of daughter cracks towards the main crack, was observed. This is most likely due to the underlaying lattice structure of our model.

For further analysis we have determined the spectrum of velocity oscillations by calculating the Fourier transform of the main crack velocity vs time. In Fig. 5 it seems that the main peak of the spectrum corresponds to the first harmonic oscillation frequency but there appears also higher harmonics, at least the second and third harmonic are clearly visible. Thus velocity oscillations are far from sinisoidal. In the figure it is also evident that there is a significant amount of white background noise in the spectrum, which, on one hand, may be due to the discreteness of the crack tip movement and, on the other hand, due to inaccuracies in the numerical algorithm. In order to improve this and facilitate noise reduction one would need larger system sizes because the model is deterministic and there is no possibility to get an ensemble average. Especially when daughter cracks are short the spectrum becomes noisy and the half-width of peaks increases.

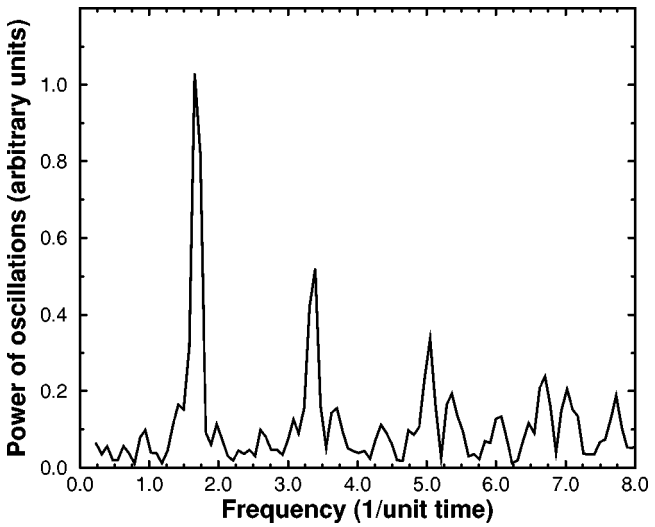

FIG. 5. Fourier spectrum of the crack tip velocity in the case of symmetric anisotropy with $k=1.3$.

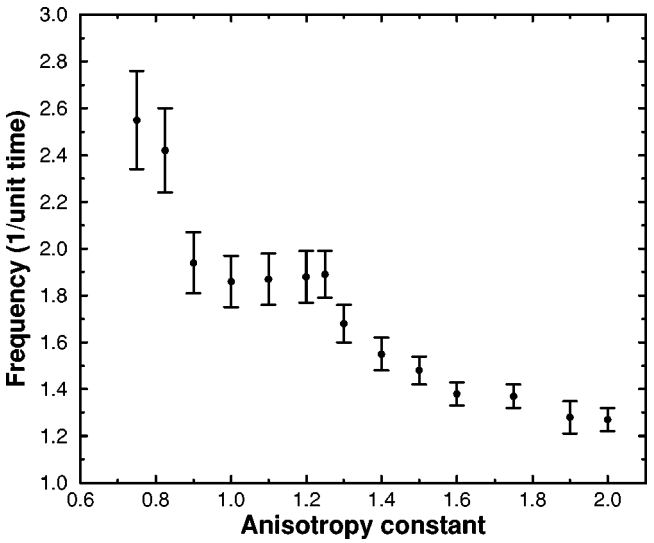

FIG. 6. First harmonic frequency of the velocity oscillation vs anisotropy. Error bars correspond to the half-width of peaks.

The frequency of daughter crack formation can also be obtained by dividing the average distance between nearest crack branches with the average speed of the crack tip. It should be noted that in this approach strictly speaking it is assumed that velocity oscillations in the propagating crack tip are exactly matching with and caused by side branching. This ''pseudo-Fourier-transform'' leads to the same result as obtained with the proper Fourier transform. Thus our results confirm with great accuracy that oscillations in crack propagation match exactly with the side branching process, similar to the experiments [8], and earlier simulations [13].

In addition, a look at the graph of the oscillation frequency of daughter crack formation vs. amount of anisotropy (Fig. 6) tells that there is no simple relation between them. If $k<0.9$ a drastic increase in frequency is observed and if $k>1.5$ a small decrease is seen. Around the $k=1$ value there is an interval where the oscillation frequency does not change much. It is interesting that although the average crack velocity is increasing, the horizontal distance between the nearest neighbor daughter cracks also increases so their combined effect causes no significant change in oscillation frequency.

B. Asymmetric anisotropy

When the special direction is *not* chosen parallel to the x direction but to an angle (here chosen to be 60°), the reflection symmetry between the two sides of the main crack will be broken. Then the most significant outcome of the symmetry breaking is the appearance of a side branching pattern with different periodicities on different sides of the main crack. If the anisotropy constant k is set greater than unity and the direction of loading is chosen in the way shown in Fig. 2(b), a denser side crack structure with short daughter cracks emerges on the lower side of the main crack. However, in this case there appear more fluctuations in the periodicity of spatial branching. On the upper side of the main crack the spatial periodicity of crack branching increases only slightly when k increases. Figure 7 shows a typical result.

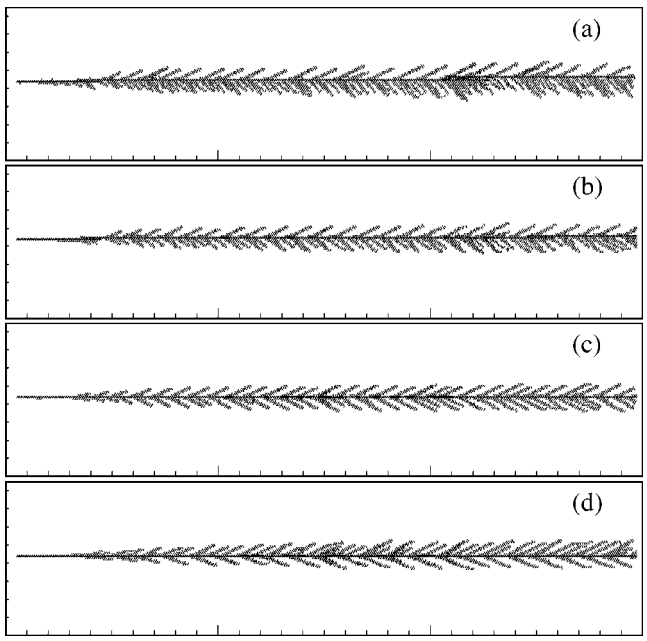

FIG. 7. Fracture pattern in case of asymmetric anisotropy: (a) $k=1.5$, (b) $k=1.3$, (c) $k=1.1$, and (d) $k=0.8$, respectively.

It is interesting to investigate in slightly more detail what happens when the anisotropy constant is varied around the isotropic condition $k=1$, in which case the spatial branching periodicity on both sides of the main crack are the same. When the anisotropy constant is raised to $k=2$, the above mentioned denser and shorter side crack structure appears. Then letting k approach the isotropic limit ($k\rightarrow 1$), the spatial periodicities of daughter cracks on both sides of the main crack tend to be the same. For example, by setting $k=1.1$ it seems that whenever a crack is formed on the upper side of the main crack there is one formed on the lower side as well. In addition to that daughter cracks are formed time to time on the lower side of the main crack between the regular branches. As $k\rightarrow 1$ less and less such irregular daughter branches are formed until finally only the regular pattern remains. Thus for small anisotropy daughter cracks appear preferably in pairs and in that way shed out rapidly extra stress from the crack tip. If the anisotropy constant is set to be less than unity the role of different sides of the main crack changes. In contrast to the symmetric case there is not any considerable dependence of the average velocity of the main crack on the anisotropy constant k.

The spectrum of crack tip velocity oscillations shows that there exists a dominant frequency as a result of daughter crack generation from that side of the propagating crack where the daughter cracks are longer. It is also quite remarkable that the spectrum peak due daughter crack oscillations of the other side is much less in height, vanishing nearly within the noise level. Thus in the instability of crack propagation longer side branches on one side of the main crack play the major role while the shorter side branches of the other side of the crack play only a minor role.

C. Disordered systems

Disorder has been introduced in the model by randomly setting the values of the spring constants of the bonds while

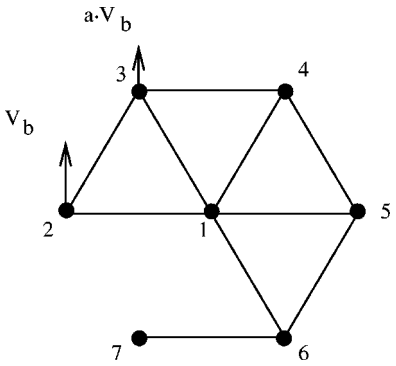

FIG. 8. A reduced model for calculating the critical crack boundary velocity.

keeping the α/β ratio constant. This kind of disorder aims to represent density fluctuations that might be the reason for local strength variation in some composite materials like paper [17]. The α values were selected according to a uniform distribution from the $(\alpha_0-\alpha_w,\alpha_0+\alpha_w)$ interval. Here α_0 is the value that has already been used for the ordered system, α_w is varied and $d=\alpha_w/\alpha_0$ is the quantity that describes the strength of disorder.

The results of such disorder are as expected. Increasing the disorder in the system makes the daughter cracks loose their regularity in length, angle, and periodicity. We have also seen that branch structure with longer daughter cracks remains more stable than the shorter branch structure. If d is greater than roughly 0.3 it is more likely that daughter cracks coalesce and instead of individual daughter cracks a hackle fracture pattern is observed. It should be underlined that velocity oscillations are far more sensitive to disorder than pattern formation, namely a small value of $d\approx 0.2$ makes the velocity oscillations of the main crack rather noisy. Then it is very difficult to obtain useful information from it. When the amount of disorder is large, i.e., $d>0.5$, voids away from the neighborhood of the crack tip are generated, but the main crack keeps its directional straightness without any significant deviations. Usually the interplay between disorder and anisotropy is interesting [as e.g., in anisotropic diffusion limited aggregation (DLA) models], and here we found that the anisotropic properties of the fracture pattern are still observable at quite a high value of disorder, up to $d=0.4$.

IV. ANALYSIS OF CRACK PATTERN FORMATION

There is a simple picture that explains how the fracture pattern might change if the system is anisotropic. Let us first assume that anisotropy has the effect that it only changes the velocity of crack propagation. Thus, in case of symmetric anisotropy one would expect that besides this increase in the velocity of the main crack, daughter cracks should elongate in the horizontal x direction and change their angle. On the other hand, the time that is needed for the daughter cracks to reach their endpoint remains the same because that is dictated by the vertical velocity component of the daughter crack away from the main crack. Assuming that the vertical length of branches is constant, this is true near the isotropic case. If we apply this picture to the asymmetric anisotropy, we expect that on one side of the main crack daughters are moving faster away from the main crack and have a greater

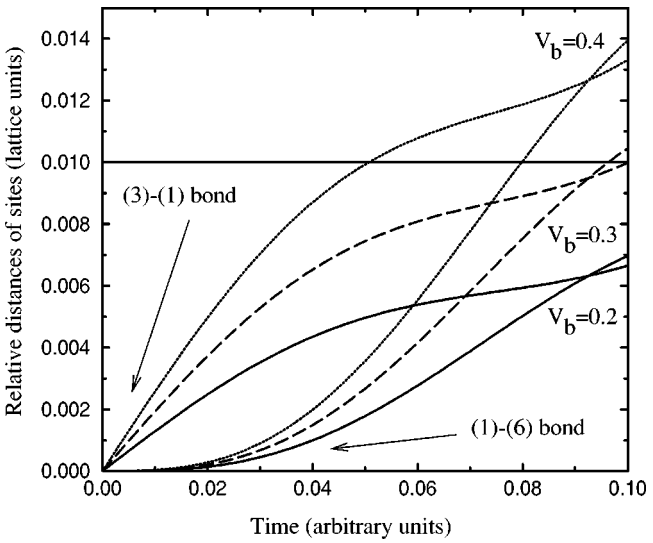

FIG. 9. Branching instability in the isotropic ($k=1$) system. In case of $v_b=0.2$ and $v_b=0.3$ (solid and dashed lines) the 1-6 bond breaks first. If $v_b=0.4$ (long-dashed line) a daughter crack starts to grow. The horizontal line represents the breaking threshold.

angle creating a densely branched pattern. The other side is less affected by the change because there the branches grow roughly perpendicularly to the direction of anisotropy.

Pattern formation and velocity oscillations of fracture are typical examples where nonlocal effects are the keys to understanding the whole phenomenon. However, in lattice models local crack tip dynamics can be understood in terms of a ''minimal model'' of an already strained triangular beam-lattice system [19,14]. This simple model can at least qualitatively describe the time dependence of the crack velocity in the case of the straightly propagating crack. However, problems arise when branching occurs. The nonlocal nature of crack propagation is that daughter cracks affect the propagation of the main crack by their screening effect, i.e., side branches cause a decrease in the stress around the crack tip. In this sense there seems to be a connection between this model and Laplacian growth models for diffusion limited aggregation (DLA) and viscous fingering [1]. In spite of the fact that Laplacian models are rotationally invariant and our model is not, the connection between them is indicated by some similarity of the governing equations and of moving boundaries, the latter including the screening effect. For more details about the relation between fracture and Laplacian growth we refer to the book edited by Herrmann and Roux [1].

In a previous publication of this model [13] it was proposed that side branching occurs if the crack boundary velocity exceeds a certain threshold velocity. By the crack boundary velocity we mean the vertical velocity of mass points at the crack tip, and it is usually considered to be proportional to the velocity of the main crack. In order to investigate analytically the effect of anisotropy on crack branching instability we studied a reduced model. It is very similar to the one used in [13], however slight modifications were done and Fig. 8 describes the main features of this model. The mass points labeled with 4, 5, 6, and 7 are fixed, whereas 2 and 3 are moving upwards with definite velocities. The velocity of site 2 is the boundary velocity v_b itself and

site 3 moves with somewhat slower velocity av_b, where the parameter a was set to 0.75. The motion of mass point 1 is calculated. Viscosity effects are omitted here because of their large time scale compared to the characteristic time of the harmonic springs. Thus nearest neighbor mass points of this model are connected simply with Born springs. With these conditions the equation of motion and its solution for mass point 1 will scale with the boundary velocity v_b. The breaking threshold of 1% is used as in the original simulation model. If the velocity of the crack boundary is small the crack propagates in a horizontal direction with a zig-zag motion via the 1-6 and then 6-5 bonds. Above a certain limiting velocity the 1-3 bond breaks first and branching emerges. Figure 9 shows the strain values of the bonds 1-6 and 1-3 in the isotropic system.

With this reduced model we have studied both cases of anisotropy, symmetric and asymmetric. In the symmetric case we find that the larger the anisotropy constant is the larger the critical velocity for crack branching is (Fig. 10), as it was observed in the simulations. In the case of asymmetric anisotropy the threshold velocities for daughter cracks on different sides of the main crack are found to be different, which is also in accordance with the simulations.

In conclusion, we can say that in our model the following scenario happens. At the beginning of loading the straight crack line moves as it is determined by the local stress. When it reaches the threshold velocity daughter cracks emerge. After propagating the distance of a few lattice constants there is a velocity decrease in the main crack due to daughter crack screening. By the time the daughter cracks are far from the main crack the screening becomes less effective and the main crack can accelerate to the velocity limit where branching occurs again. Thus oscillations in the velocity of the main crack are seen. As for oscillation frequency and regularity, this picture changes due to anisotropy and disorder in the system.

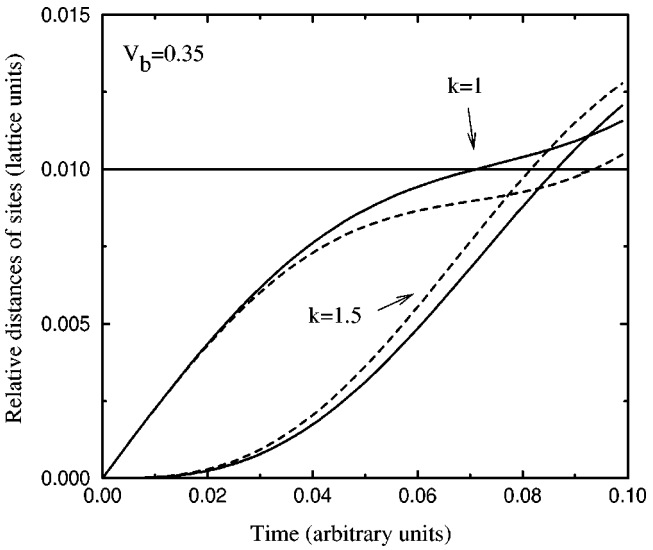

FIG. 10. Effect of symmetric anisotropy on crack branching. Increasing the anisotropy constant increases the critical crack velocity for branching. For the crack boundary velocity shown, branching occurs for $k=1$, but does not occur for $k=1.5$.

V. SUMMARY

We have studied the role of anisotropy and disorder in the viscoelastic model, with Born springs and Maxwell-type viscous dashpots. Even though our results are qualitative and restricted to a certain lattice structure it clearly shows the effects of anisotropy on fracture. In the case of symmetric anisotropy the average velocity of the main crack, the length of the cracks and their periodicity changes as a function of the anisotropy constant. The most interesting part of our results is that in the case of asymmetric anisotropy there exists two quantitatively different periodic structures in the fracture pattern. When disorder in terms of the spring constant is implemented to the model, fluctuations in the crack tip velocity and in the branch structure are seen, but the main effects of anisotropy remain unchanged.

ACKNOWLEDGMENTS

This work was in part supported by OTKA (T29985), FKFP (30/1999), and the Academy of Finland.

[1] *Statistical Models for the Fracture of Disordered Media*, edited by H. J. Herrmann and S. Roux (North-Holland, Amsterdam, 1990).
[2] A. Yuse and M. Sano, Nature (London) **362**, 329 (1993).
[3] J. Kertész, V. K. Horváth, F. Weber, Fractals **1**, 67 (1993).
[4] K. Ravi-Chandar and W. G. Knauss, Int. J. Fract. **26**, 141 (1984).
[5] L. B. Freund, *Dynamic Fracture Mechanics* (Cambridge University Press, New York, 1990).
[6] E. H. Yoffe, Philos. Mag. **42**, 739 (1951).
[7] J. Fineberg, S. P. Gross, M. Marder, H. Swinney, Phys. Rev. B **45**, 5146 (1992).
[8] E. Sharon, S. P. Gross, and J. Fineberg, Phys. Rev. Lett. **76**, 2117 (1996).
[9] J. F. Boudet and S. Ciliberto, Phys. Rev. Lett. **80**, 341 (1998); J. F. Boudet, S. Ciliberto, and V. Steinberg, Europhys. Lett. **30**, 337 (1995).
[10] R. Blumenfeld, Phys. Rev. Lett. **76**, 3703 (1996).
[11] M. Marder and X. Liu, Phys. Rev. Lett. **71**, 2417 (1993).
[12] F. F. Abraham, D. Brodbeck, R. A. Rafey, and W. E. Rudge, Phys. Rev. Lett. **73**, 272 (1994).
[13] P. Heino and K. Kaski, Phys. Rev. B **54**, 6150 (1996).
[14] J. Åström, M. Alava, and J. Timonen, Phys. Rev. E **57**, R1259 (1998).
[15] M. Born and K. Huang, *Dynamical Theory of Crystal Lattices* (Oxford University Press, New York, 1954).
[16] G. N. Hassold and D. J. Srolovitz, Phys. Rev. B **39**, 9273 (1989).
[17] P. Heino, K. Kaski, Phys. Rev. E **56**, 4364 (1997).
[18] T. T. Rautiainen, M. J. Alava, and K. Kaski, Phys. Rev. E **51**, R2727 (1995).
[19] B. L. Holian, R. Blumenfeld, P. Gumbsch, Phys. Rev. Lett. **78**, 78 (1997).